CARBON 52 (2013) 347–355

Available at www.sciencedirect.com

SciVerse ScienceDirect

journal homepage: www.elsevier.com/locate/carbon

Stress relaxation in carbon nanotube-based fibers for load-bearing applications

Mei Zu [a,b], *Qingwen Li* [c], *Yuntian Zhu* [d], *Yong Zhu* [e], *Guojian Wang* [a], *Joon-Hyung Byun* [f], *Tsu-Wei Chou* [b,*]

[a] *School of Materials Science and Engineering, Tongji University, Shanghai 201804, China*
[b] *Department of Mechanical Engineering and Center for Composite Materials, University of Delaware, Newark, DE 19716, USA*
[c] *Suzhou Institute of Nano-Tech and Nano-Bionics, Suzhou 215123, China*
[d] *Department of Materials Science and Engineering, North Carolina State University, Raleigh, NC 27695, USA*
[e] *Department of Mechanical and Aerospace Engineering, North Carolina State University, Raleigh, NC 27695, USA*
[f] *Composites Research Center, Korean Institute of Materials Science, Changwon 641831, South Korea*

ARTICLE INFO

Article history:
Received 8 June 2012
Accepted 17 September 2012
Available online 25 September 2012

ABSTRACT

Carbon nanotube (CNT) based continuous fiber, a CNT assembly that could retain the superb properties of individual CNTs on a macroscopic scale, has emerged as a promising candidate for reinforcement in multifunctional composites. While existing research has extensively examined their short-term mechanical properties based upon quasi-static measurements, the long-term durability of CNT fibers has been largely neglected. Here we report time-dependent behavior of CNT fibers, with a particular focus on tensile stress relaxation. Both the pure CNT fiber and the CNT/epoxy composite fiber exhibited significant stress decay during the relaxation process, and this time-dependent behavior became more significant at a higher initial strain level, a lower strain rate and a greater gauge length. The present approach signifies a fundamental difference in the load-bearing characteristics between CNT fibers and traditional advanced fibers, which has major implications for the long-term durability of CNT fibers in load-bearing multifunctional applications.

1. Introduction

Since their successful processing in 2000 [1], carbon nanotube-based continuous fibers have been extensively studied. The established methods of producing CNT fibers, namely, spinning from CNT solution [1], spinning from a vertically aligned CNT array previously grown on a substrate [2,3], spinning from a CNT aerogel formed in a chemical vapor deposition reactor [4], and twisting/rolling from a CNT film [5], enable translation of the remarkable mechanical, electrical and thermal properties of individual carbon nanotubes to the macroscopic scale. Comprehensive reviews of the fabrication and performance of CNT fibers have been provided in several papers published in recent years [6–9].

As a fundamental subject of research, the mechanical properties of CNT fibers have attracted considerable attention, particularly their tensile [10,11], compressive [12,13] and CNT fiber/polymer matrix interfacial performance [14,15]. Single-fiber quasi-static tensile tests have been adopted as the most common technique for characterizing their mechanical properties. With continuous improvement in their tensile strength and Young's modulus owing to

* *Corresponding author:* Fax: +1 302 831 3619.
E-mail address: chou@udel.edu (T.-W. Chou).
0008-6223/$ - see front matter
http://dx.doi.org/10.1016/j.carbon.2012.09.036

extensive worldwide efforts, CNT fibers have great potential for reinforcement in multifunctional composites. To enable a comprehensive assessment of the full potential of CNT fibers and to identify the needs of future research, it is imperative that we move beyond the investigation of short-term CNT fiber mechanical properties based upon quasi-static measurements. The following introduces the motivation for the study of one aspect of the long-term mechanical performance of CNT fibers.

An interesting phenomenon was observed in our recent tensile recoil experiments for an indirect measurement of CNT fiber compressive strength [13]. In this experiment, after a static tensile load was applied and held at a level below the failure load, the fiber recoil was initiated by cutting the specimen at the midpoint of its gauge length. Unlike in the tensile recoil tests of traditional advanced fibers such as Kevlar and carbon fiber [16], it was not feasible to hold the CNT fiber at the initial load level and a load (or stress) decay was observed when the fiber was held at the constant strain. This observation indicates that there exists a fundamental difference in the load-bearing performances between CNT fibers and traditional advanced fibers. An example of time-dependent behavior can be found in the recent work of Wu et al. [17], who examined the electrical resistance-stress hysteresis behavior of pure CNT fibers under quasi-static cyclic tensile loading. A time-dependent behavior relevant to CNT-based composite fibers was reported by Ma et al. [18]. Using dynamic mechanical tests, they examined the creep and creep recovery behavior of PVA/CNT composite fibers. The nature of such a problem is similar to that of a short-fiber reinforced polymeric composite [19].

In this paper we conduct a comprehensive study of the various factors affecting the tensile stress relaxation behavior of CNT fibers. We found that higher initial strain level, lower strain rate, and greater gauge length resulted in a higher rate of stress decay in both pure fiber and composite fiber. The sliding among the numerous short CNTs, which are held together mostly by van der Waals interactions, is the primary source of time-dependent deformation of CNT-based continuous fibers. Better understanding of the stress relaxation mechanism of CNT fibers is imperative for minimizing their relaxation behavior in the future.

2. Experimental

2.1. Preparation of CNT fibers

CNT fibers tested in this study were spun by drawing and twisting of CNT strips out of vertically well-aligned CNT arrays (forests), whose CNTs were super-aligned and mainly double- and triple-walled with diameters of ~6 nm. Specific details of the preparation of CNT fibers can be found in Reference [20]. The weight of CNT fibers was measured on an Ultra-microbalance (METTLER TOLEDO XP2U). A typical 13 μm diameter and 100 mm long CNT fiber weighed 10–30 μg, giving a linear density between 0.1–0.3 tex (1 tex = 1 μg/mm). CNT/epoxy composite fibers were prepared using a soaking technique [13,21].

2.2. Single-fiber tensile tests

Details of the specimen preparation for single-fiber tensile tests can be found elsewhere [15]. Ten specimens of each type of fiber were tested on a Shimadzu EZ-S testing machine with a load cell of 2N and a strain rate of $5.5 \times 10^{-4}\,s^{-1}$. The gauge length of all specimens was fixed to 15 mm, and their diameters were measured by the laser diffraction method.

2.3. Tensile stress relaxation tests

The specimen fabrication technique and the testing equipment used in the tensile stress relaxation experiments were the same as those used in quasi-static tensile measurements. The ultimate strain values of both pure and composite fibers, obtained from the quasi-static tensile tests, were used as the reference strain level to determine the applied strain in the relaxation tests. To investigate the effects of the initial strain level, strain rate and gauge length on the tensile relaxation behavior of CNT fibers, specimens with two gauge lengths, namely, 7 and 15 mm, were deformed to several strain levels, namely, 0.5%, 1.0%, 1.5% and 2.0% at different strain rates, namely, 5.5×10^{-5}, 5.5×10^{-4} and $5.5 \times 10^{-3}\,s^{-1}$. Upon reaching the predetermined initial strain (ε_0), the specimen was then held at this strain level, and the force (F) needed to sustain the constant strain was monitored and recorded by a digital camera for a time span of 1 h. Specimens of single carbon fiber were also tested for comparison. All stress relaxation tests were performed at room temperature. In our previous work [15], statistical analysis using a two-parameter Weibull distribution model shows that the CNT fibers from the same source as the current fibers have small scattering in their strengths, indicating high quality consistency of these fibers. Therefore, in this study, five specimens of each type of fibers were tested for each given condition (tensile rate, initial strain level and gauge length) and the specimen whose testing result was closest to the average value of the five sets of data was selected as the representative at each given condition for following analysis. The results of stress relaxation were plotted with the stress ratio (σ_t/σ_0) obtained from the stress at a specific time (σ_t) divided by the maximum stress (σ_0) when the required strain was attained versus log time; or the stress relaxation modulus at a particular time ($E_t = \sigma_t/\varepsilon_0$) against the logarithm of time. The stress was calculated under the assumption that there was no change in the cross-sectional area of the specimen during the relaxation tests. The slope of the plotted curve (designated as S in all the figures) was obtained by a regression analysis of the data for the best fit to a straight line.

2.4. In-situ Raman measurements

In-situ Raman measurements during fiber loading and relaxation were carried out using a LabRAM HR (Jobin–Yvon, Horiba Group, France) microspectrometer in conjunction with a confocal microscope. The laser with a wavelength of 632.81 nm was used to excite Raman scattering in the

specimen. The spectra were taken with a 100× objective lens, which gives a laser spot size of around 1 micron. The laser power was adjusted to 2 mW to avoid the heating effect. The exposure time was set at 5 s, and an accumulation number of three times was used. Before testing, the instrument was calibrated with the 520 cm^{-1} peak of silicon substrate. A tensile-testing stage (Ernest F. Fullam) was used to deform the CNT fibers under the microscope. The tensile rate was set at 2.3 mm/min. The peak values were derived by using Lorentzian routines fitted to the raw data obtained from the spectrometer.

3. Results and discussion

3.1. *Tensile properties of CNT fibers*

The typical tensile stress–strain curves of CNT fibers before and after epoxy resin infiltration are illustrated in Fig. 1a. For comparison, a single carbon fiber (T-300) specimen with a diameter of 7 μm was also tested. It can be seen from Fig. 1a that both pure CNT fiber and CNT/epoxy composite fiber had a higher strain-to-failure than that of the carbon fiber, even though their tensile strengths and Young's moduli were

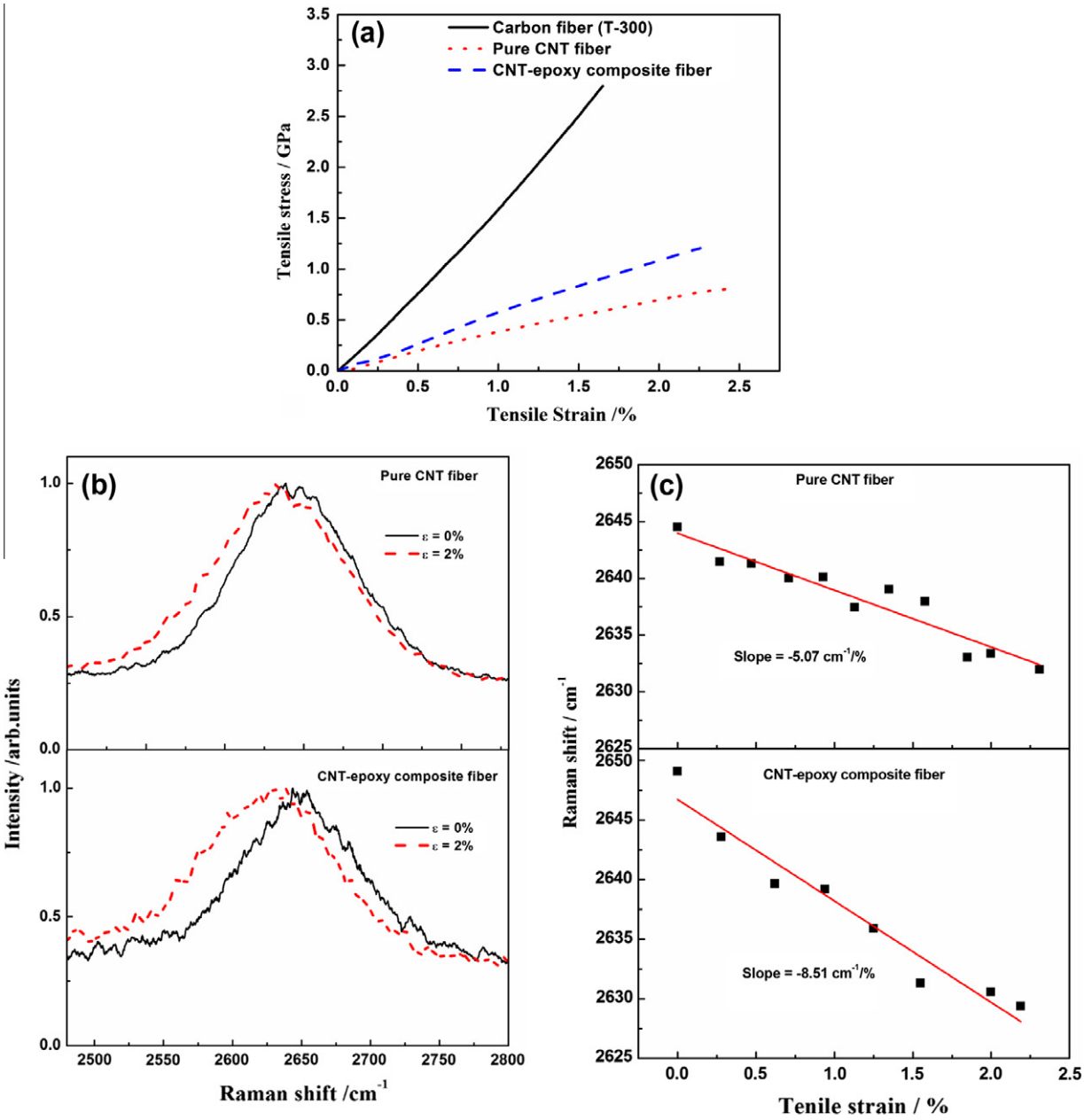

Fig. 1 – Single-fiber quasi-static tensile tests of CNT fibers. (a) Typical tensile stress–strain curves of carbon fiber, pure CNT fiber and CNT/epoxy composite fiber. (b) Typical G' band Raman spectra of a pure CNT fiber and a CNT/epoxy composite fiber at the tensile strains of 0% and 2%. (c) Raman peak shift of the G' band as a function of applied strain.

much lower than those of the carbon fiber. Due to resin infiltration, the diameter of the CNT fiber was slightly increased from 13 to 14 μm. However, after resin infiltration, the tensile strength of CNT fibers increased from 0.8 to 1.2 GPa, and the Young's modulus increased from 44 to 62 GPa, while the strain to failure decreased slightly from 2.5% to 2.2%. This enhancement in mechanical performance of the CNT/epoxy composite fiber is attributed to the effective infiltration of the epoxy resin into the void space within the pure CNT fiber, which was confirmed by the microscopic images in our previous study [13]. However, it should be noted that the tensile strength and modulus of CNT fibers tested in this study were lower than those of our previous work [13,15], which could be attributed to the larger fiber diameter and greater gauge length adopted in the present study.

The enhancement in mechanical performance of the CNT/epoxy composite fiber, indicating the increase in the load transfer to the CNTs after resin infiltration, is further verified by *in-situ* Raman measurements during the fiber deformation process. Fig. 1b shows typical G' band Raman spectra of a pure CNT fiber and a CNT/epoxy composite fiber under strain. The major characteristic of both types of specimen is the downshifting trend of the peak position and the broadening of the line shape. The downshifts of the G' band are expected and arise as a result of the elongated carbon–carbon bonds [22,23]. The variation of the peak positions is summarized in Fig. 1c. Unlike the two-stage feature of downshifts of the G' band observed at low and high strains in other CNT fiber-related studies [5,18], the downshifts of the G' band in this study showed a monotonic increase with rates of 5.07 and 8.51 cm^{-1} per 1% strain for the pure fiber and CNT/epoxy composite fiber, respectively. The elevated downshift rate of G' Raman band could be attributed to the improved strain transfer efficiency with the introduction of the epoxy matrix. This implied that more load was carried by CNTs in the composite fiber than in the pure fiber at a given macroscale strain. It should be noted that the downshift rate of the G' band for the fibers studied here is different from those reported in other studies [5,18,24], probably due to the variation in the composition and structure of CNT fibers tested.

3.2. Comparisons of tensile stress relaxation behavior of different fibers

Specimens of carbon fiber, pure CNT fiber and CNT/epoxy composite fiber were stretched to an initial strain level of 1.0% at a constant strain rate of $5.5 \times 10^{-4}\ s^{-1}$, and their stress relaxation data are plotted in Fig. 2. As can be seen from the force–time curves shown in Fig. 2a, the load of the carbon fiber was almost constant after 1 h and decreased by only 5.4% even after being held for 18 h at the constant initial strain. As for pure CNT fiber, there was significant load decay during the first four minutes of the relaxation process, and the load dropped by as much as 32% after 18 h at constant strain. This divergence in the relaxation behavior of carbon fiber and pure CNT fiber is a reflection of their structural differences. Unlike the dense structure of carbon fiber, a single CNT fiber is an assembly of individual CNTs held together by weak van der Waals force, limited mechanical interlocking, and friction force [11]. When the CNT fiber was held at a constant strain, slippage among CNT bundles within the fiber took place. This sliding could be a time- and load-dependent phenomenon, which resulted in a gradual load drop. Fig. 2b presents the stress relaxation plot of stress ratio σ_t/σ_0 versus time of the three specimens. It is noted that the stress relaxation rate of the composite fiber, as represented by the slope of the curve, was higher than that of the pure fiber at the same initial strain level, even though the composite fiber retained a higher load after 1 h. According to the previous studies on interfacial properties between CNT fibers and polymer resins [14,15], the critical interfacial shear strength for the onset of slip at the CNT/epoxy interface was only in the range of 12–20 MPa, which suggested that the interaction between the CNT fiber and epoxy matrix was insufficient. However, the initial stress of the composite fiber, calculated from the initial force reached at 1% strain, was around 400 MPa. Therefore, one possible mechanism for the observed increase in the composite fiber relaxation rate is that in addition to interbundle sliding, CNT/epoxy interfacial sliding may occur during the relaxation process.

3.3. Various effects on the tensile stress relaxation behavior of CNT fibers

3.3.1. Effect of initial strain level

Fig. 3 presents the stress relaxation plot with both the force (F) and the stress relaxation modulus (E_t) versus time of CNT fibers and their composites at several initial strain levels, namely 0.5%, 1.0%, 1.5% and 2.0% at the constant strain rate of $5.5 \times 10^{-4}\ s^{-1}$. Compared to that of pure CNT fiber, a higher initial load and greater load retention after 1 h were observed in the case of CNT/epoxy composite fiber at each initial strain level (Fig. 3a and b). In addition, it was obvious from Fig. 3c that the rate of stress relaxation of pure CNT fiber increased gradually with the initial strain level. The higher rate of relaxation occurring at elevated initial strain level could be attributed to the larger amount of permanent deformation resulting from the irreversible slippage among CNT bundles within the fiber. A similar tendency in the relaxation rate variation with the initial strain level was observed in the composite fiber (Fig. 3d).

3.3.2. Effect of strain rate

To explore the effect of tensile strain rate on the relaxation behavior of CNT fibers, specimens of both CNT fiber and composite fiber were loaded to the initial strain of 1.0% with two different strain rates, namely, 5.5×10^{-5} and $5.5 \times 10^{-3}\ s^{-1}$. Higher initial tensile stress and modulus were observed in both the pure CNT fiber and its composite fiber when a higher strain rate was applied (Fig. 4a and b). From the slope of the curves shown in Fig. 4c and d, we found that the stress relaxation rate was inversely proportional to the tensile strain rate. Although the differences among the sample testing results at the two strain rates shown in Fig. 4 are not great, a higher slope value at the lower strain rate was observed in all the five testing sets. It is likely due to the fact that when a lower tensile rate was applied to the fiber, CNT bundles within the fiber had adequate time to slip past each other and adjust their alignment in the tensile direction, resulting in irreversible deformation, whereas when the fiber was deformed at a

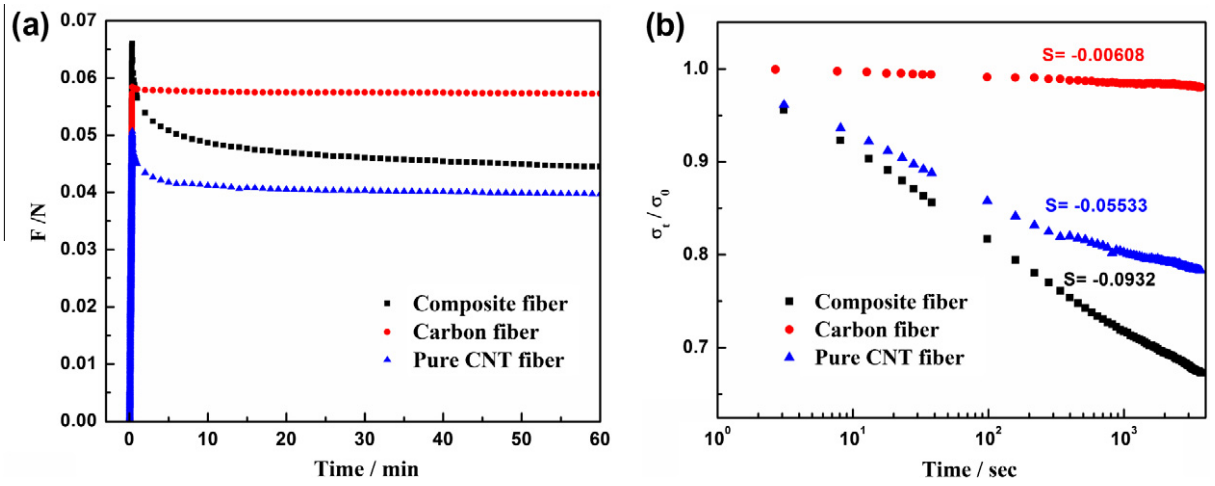

Fig. 2 – Comparisons of relaxation behavior of carbon fiber, pure CNT fiber and CNT/epoxy composite fiber. (a) Force as a function of time during loading and relaxation. (b) Stress ratio σ_t/σ_0 as a function of time.

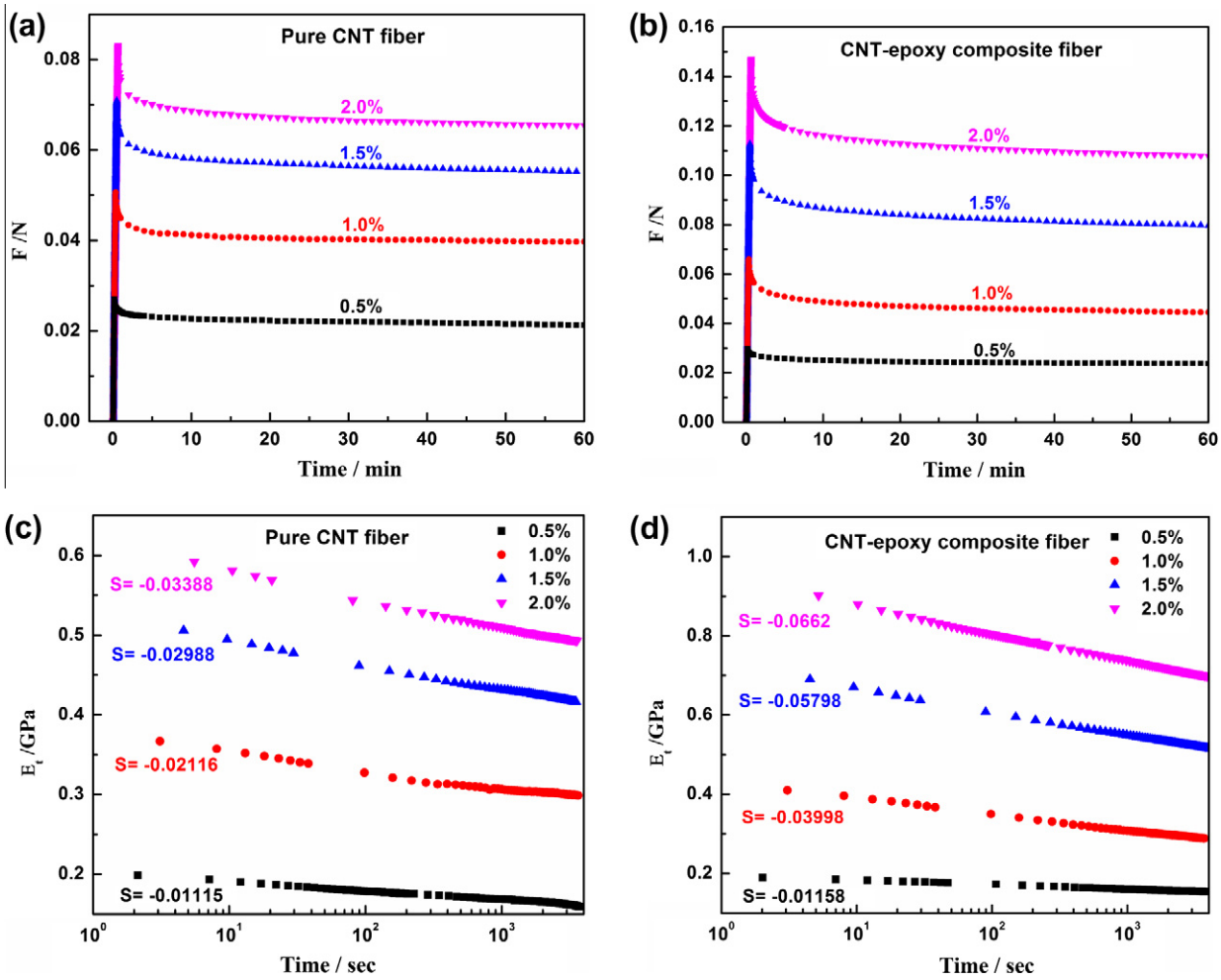

Fig. 3 – Effect of initial strain level on the relaxation behavior of CNT fibers. Force as a function of time during the loading and relaxation of (a) pure CNT fiber and (b) CNT/epoxy composite fiber. Stress relaxation modulus E_t as a function of time of (c) pure CNT fiber and (d) CNT/epoxy composite fiber.

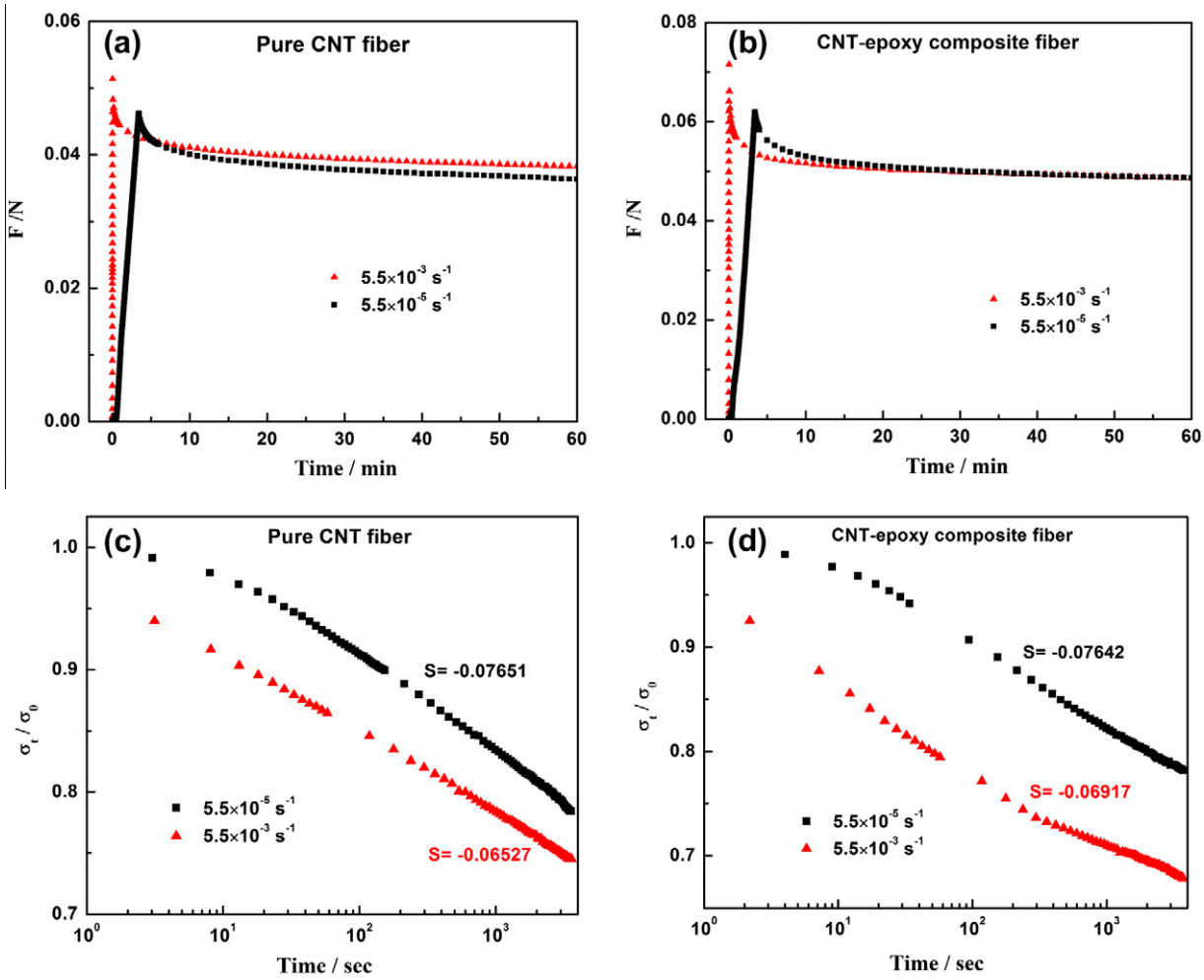

Fig. 4 – Effect of strain rate on the relaxation behavior of CNT fibers. Force as a function of time during the loading and relaxation of (a) the pure CNT fiber and (b) the CNT/epoxy composite fiber. Stress ratio σ_t/σ_0 as a function of time of (c) the pure CNT fiber and (d) the CNT/epoxy composite fiber.

higher strain rate, much of the fiber deformation was elastic and reversible. Therefore, elastic recovery occurred during the relaxation stage of the fiber loaded with a higher strain rate, and thus a lower relaxation rate was expected.

3.3.3. *Effect of gauge length*

The effect of gauge length on the stress relaxation behavior was investigated for specimens with two different gauge lengths, namely, 7 and 15 mm. The specimens were loaded to the initial strain of 1.0% at the constant strain rate of $5.5 \times 10^{-4}\,s^{-1}$. Fig. 5 shows that in both cases, *i.e.*, pure fiber and composite fiber, the initial force and the initial stress relaxation modulus of the specimen with greater gauge length were higher than those with lower gauge length when the same initial strain was attained. After a time span of 1 h, the stress relaxation modulus retention of the former was still higher than that of the latter. However, it is shown in Fig. 5c and d that the 15-mm specimen exhibited a higher relaxation rate than the 7-mm specimen. This gauge length-dependent behavior was even more obvious in the case of CNT/epoxy composite fiber (Fig. 5d). This behavior is consistent with the size effect observed in traditional advanced fibers [19]. Specimens with greater gauge length have a higher probability of defects, resulting in higher local stress concentration, and hence larger extent of irreversible deformation and stress relaxation of the fiber.

3.4. *Raman characterization during CNT fiber relaxation*

To investigate the mechanism that could be responsible for the observed stress decay of CNT fibers, *in-situ* Raman measurements were carried out during fiber relaxation process. A specimen of pure CNT fiber was stretched to an initial strain of 1.67%. After being held for 16 h under this initial strain, the specimen was tensile loaded until failure. Variation of the G' band peak position during the relaxation process is shown in Fig. 6. As expected, the G' band peak position had a downshift when the specimen was stretched to the initial strain of 1.67%. This downshift continued until failure at a strain around 2.3%, indicating the deformation of CNTs due to the applied stress. However, there was no obvious trend of the variation of the G' band peak position with an increase in the duration of the relaxation process. Since Raman scattering is sensitive to the inter-atomic distance when CNTs are mechanically strained

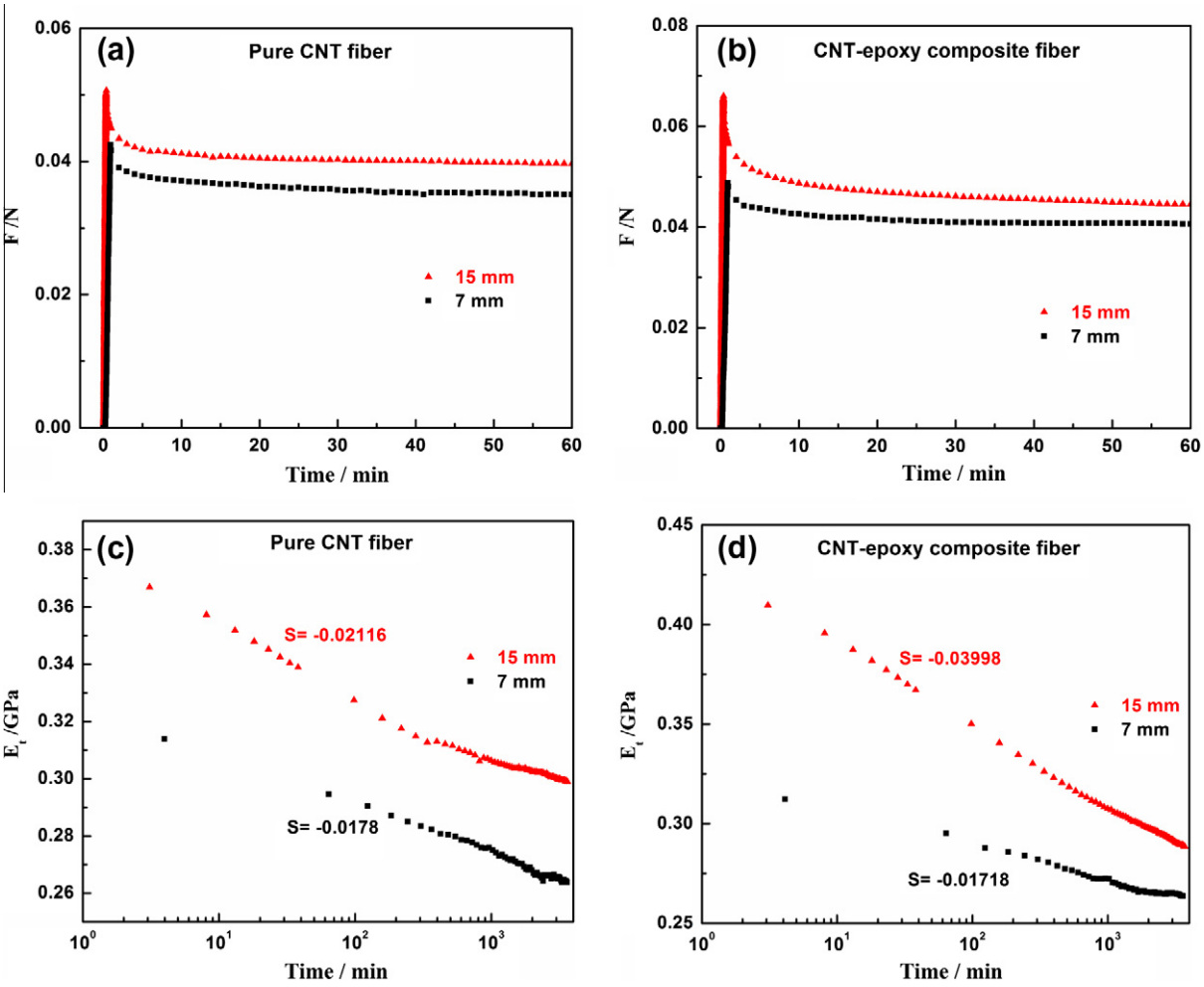

Fig. 5 – Effect of gauge length on the relaxation behavior of CNT fibers. Force as a function of time during the loading and relaxation of (a) pure CNT fiber and (b) CNT/epoxy composite fiber. Stress relaxation modulus E_t as a function of time of (c) pure CNT fiber and (d) CNT/epoxy composite fiber.

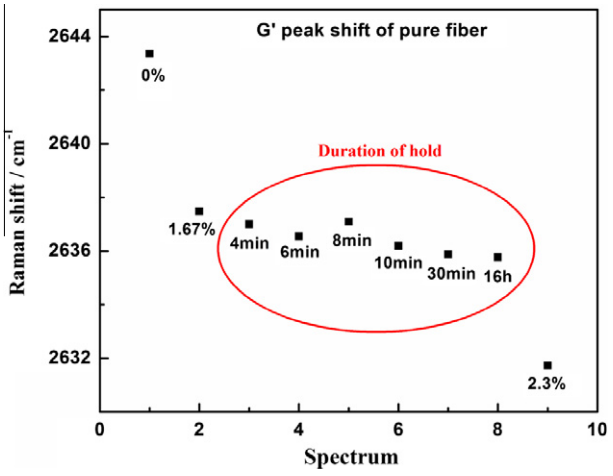

Fig. 6 – Variation of the G' band peak position with increase in the duration of relaxation for the pure fiber.

[22,23], this observation in Raman characterization implies that the stress relaxation of the CNT fiber observed in the relaxation tests could largely arise from slippage among CNT bundles.

3.5. *Simulation of the relaxation behavior*

The stretched exponential function is used to simulate the relaxation behavior of CNT fibers and the mathematical expression of this function is given in Eq. (1) [25]

$$E(t) = (E_0 - E_\infty)e^{-\left(\frac{t}{\tau}\right)^k} + E_\infty (0 < k < 1) \quad (1)$$

This function expresses the tensile stress relaxation modulus $E(t)$ as a function of the time t during the relaxation. There are four parameters in this function, namely, the initial tensile modulus E_0, the equilibrium tensile relaxation modulus E_∞, the relaxation time τ and the distribution parameter k. The predicted curves of the stress relaxation of pure CNT fiber and CNT/epoxy composite fiber at several strain levels using the stretched exponential function as well as the experimental data are shown in Fig. 7. The values of k were found to be about 0.40 for both pure CNT fiber and CNT/epoxy composite fiber at all strain levels and hence $k = 0.40$ was used for all simulations. It can be seen that the stretched exponential function fits the experimental stress relaxation data very well for both pure CNT fiber and CNT/epoxy composite fiber. The values of the stress relaxation model parameters are given

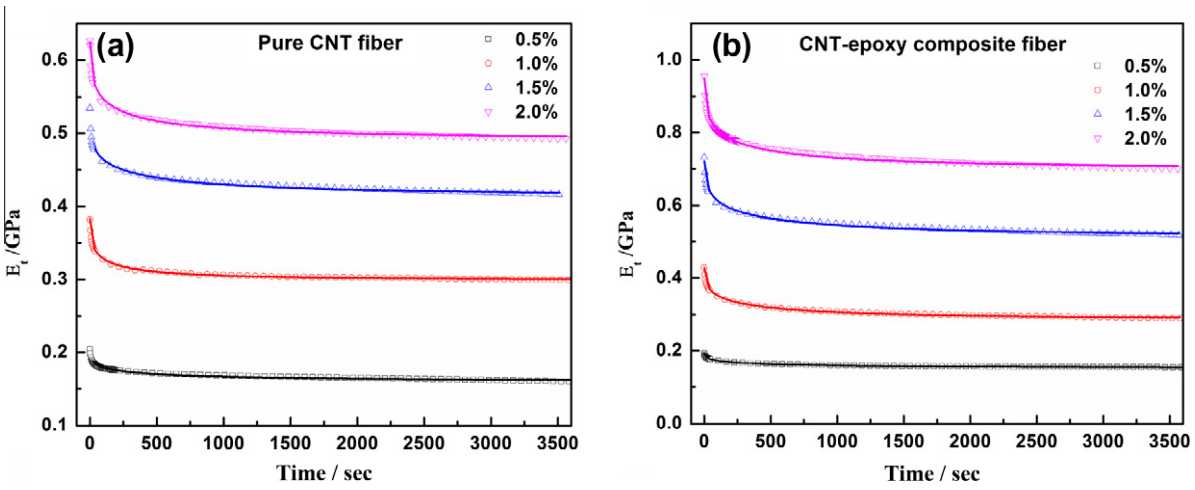

Fig. 7 – Stress relaxation curves predicted from the stretched exponential model for (a) the pure CNT fiber and (b) the CNT/epoxy composite fiber. Symbols are experimental data and solid lines are the predicted curves.

Table 1 – Summary of the stretched exponential model parameters for both the pure CNT fiber and the composite fiber.

Initial strain level (%)	E_0–E_∞ (GPa)		τ (s)		E_0 (GPa)		E_∞ (GPa)	
	Pure	Composite	Pure	Composite	Pure	Composite	Pure	Composite
0.5	0.04	0.04	251.6	290.5	0.20	0.19	0.16	0.15
1.0	0.08	0.14	86.7	196.7	0.38	0.43	0.30	0.33
1.5	0.11	0.21	205.5	212.1	0.52	0.72	0.41	0.51
2.0	0.13	0.25	135.4	150.4	0.62	0.95	0.49	0.70

in the Table 1. It is noted that for both pure fiber and composite fiber, the initial modulus E_0 simulated by the function was almost the same as the experimental value at each initial strain level. Furthermore, at each strain level, the composite fiber had higher relaxation time and retained greater equilibrium modulus compared to those of pure fiber (except at 0.5% initial strain).

4. Conclusion

This paper reports a comprehensive study of the various factors affecting the tensile stress relaxation behavior of CNT fibers, including the fiber type, initial strain level, strain rate and gauge length. The major conclusions are as follows. First, both the pure CNT fiber and the CNT/epoxy composite fiber exhibited significant stress decay during the relaxation process, whereas no obvious stress relaxation was observed in the case of the single carbon fiber. Second, higher initial strain level, lower strain rate, and greater longer gauge length resulted in a higher rate of stress decay in both the pure fiber and the composite fiber. Third, due to interfacial sliding at the CNT/epoxy interface as well as interbundle sliding, the composite fiber showed a higher relaxation rate than that of the pure fiber with the same initial strain, although the former retained a higher stress relaxation modulus after a holding time of 1 h.

On account of the stress relaxation mechanisms of CNT fibers, the present research points out that future effort in minimizing the relaxation behavior should focus on enhancing interactions among CNT bundles in the pure fiber and improving resin infiltration as well as enhancing interfacial bonding between CNT bundles and the resin in the composite fiber. The present approach has demonstrated the significant implication of time-dependent behavior in general and tensile stress relaxation in particular on the long-term durability of CNT fiber based load-bearing multifunctional composites.

Acknowledgments

This work was partially supported by the US Air Force Office of Scientific Research (Dr. Byung-Lip Lee, Program Director), the National Research Foundation of Korea (NRF) through a grant provided by the Korean Ministry of Education, Science and Technology (MEST) and the Office of Naval Research (Dr. Yapa Rajapakse, Program Director). The authors thank Dr. Weibang Lu for useful discussions on fiber relaxation testing results. The assistance and advice of Xin Wang and Feng Xu in fiber tensile testing methodology as well as Raman characterization are also greatly appreciated. Mei Zu's study abroad at the University of Delaware is supported by the State Scholarship Fund of the China Scholarship Council.

REFERENCES

[1] Vigolo B, Penicaud A, Coulon C, Sauder C, Pailler R, Journet C, et al. Macroscopic fibers and ribbons of oriented carbon nanotubes. Science 2000;290(5495):1331–4.

[2] Jiang KL, Li QQ, Fan SS. Nanotechnology: spinning continuous carbon nanotube yarns – carbon nanotubes weave their way into a range of imaginative macroscopic applications. Nature 2002;419(6909):801.

[3] Zhang XF, Li QW, Holesinger TG, Arendt PN, Huang JY, Kirven PD, et al. Ultrastrong, stiff, and lightweight carbon-nanotube fibers. Adv Mater 2007;19(23):4198–201.

[4] Li YL, Kinloch IA, Windle AH. Direct spinning of carbon nanotube fibers from chemical vapor deposition synthesis. Science 2004;304(5668):276–8.

[5] Ma WJ, Liu LQ, Yang R, Zhang TH, Zhang Z, Song L, et al. Monitoring a micromechanical process in macroscale carbon nanotube films and fibers. Adv Mater 2009;21(5):603–8.

[6] Behabtu N, Green MJ, Pasquali M. Carbon nanotube-based neat fibers. Nano Today 2008;3(5–6):24–34.

[7] Chou T-W, Gao LM, Thostenson ET, Zhang ZG, Byun JH. An assessment of the science and technology of carbon nanotube-based fibers and composites. Compos Sci Technol 2010;70(1):1–19.

[8] Liu L, Ma W, Zhang Z. Macroscopic carbon nanotube assemblies: preparation, properties, and potential applications. Small 2011;7(11):1504–20.

[9] Lu W, Zu M, Byun J-H, Kim B-S, Chou T-W. State of the art of carbon nanotube fibers: opportunities and challenges. Adv Mater 2012;24(14):1805–33.

[10] Wu AS, Nie X, Hudspeth MC, Chen WW, Chou T-W, Lashmore D, et al. Strain rate-dependent tensile properties and dynamic electromechanical response of carbon nanotube fibers. Carbon 2012;50(10):3876–81.

[11] Sabelkin V, Misak HE, Mall S, Asmatulu R, Kladitis PE. Tensile loading behavior of carbon nanotube wires. Carbon 2012;50(7):2530–8.

[12] Gao Y, Li J, Liu L, Ma W, Zhou W, Xie S, et al. Axial compression of hierarchically structured carbon nanotube fiber embedded in epoxy. Adv Funct Mater 2010;20(21):3797–803.

[13] Zu M, Lu W, Li QW, Zhu Y, Wang G, Chou T-W. Characterization of carbon nanotube fiber compressive properties using tensile recoil measurement. ACS Nano 2012;6(5):4288–97.

[14] Deng F, Lu WB, Zhao HB, Zhu YT, Kim BS, Chou T-W. The properties of dry-spun carbon nanotube fibers and their interfacial shear strength in an epoxy composite. Carbon 2011;49(5):1752–7.

[15] Zu M, Li Q, Zhu Y, Dey M, Wang G, Lu W, et al. The effective interfacial shear strength of carbon nanotube fibers in an epoxy matrix characterized by a microdroplet test. Carbon 2012;50(3):1271–9.

[16] Allen SR. Tensile recoil measurement of compressive strength for polymeric high-performance fibers. J Mater Sci 1987;22(3):853–9.

[17] Wu AS, Chou T-W, Gillespie Jr JW, Lashmore D, Rioux J. Electromechanical response and failure behaviour of aerogel-spun carbon nanotube fibres under tensile loading. J. Mater. Chem. 2012;22(14):6792–8.

[18] Ma WJ, Liu LQ, Zhang Z, Yang R, Liu G, Zhang TH, et al. High-strength composite fibers: realizing true potential of carbon nanotubes in polymer matrix through continuous reticulate architecture and molecular level couplings. Nano Lett 2009;9(8):2855–61.

[19] Chou T-W. Microstructural design of fiber composites. Cambridge: Cambridge University Press; 1992. p. 169–227.

[20] Jia JJ, Zhao JN, Xu G, Di JT, Yong ZZ, Tao YY, et al. A comparison of the mechanical properties of fibers spun from different carbon nanotubes. Carbon 2011;49(4):1333–9.

[21] Bogdanovich AE, Bradford PD. Carbon nanotube yarn and 3-D braid composites. Part I: tensile testing and mechanical properties analysis. Compos Part A 2010;41(2):230–7.

[22] Cronin SB, Swan AK, Unlu MS, Goldberg BB, Dresselhaus MS, Tinkham M. Measuring the uniaxial strain of individual single-wall carbon nanotubes: resonance Raman spectra of atomic-force-microscope modified single-wall nanotubes. Phys Rev Lett 2004;93(16):167401.

[23] Cronin SB, Swan AK, Unlu MS, Goldberg BB, Dresselhaus MS, Tinkham M. Resonant Raman spectroscopy of individual metallic and semiconducting single-wall carbon nanotubes under uniaxial strain. Phys Rev B 2005;72(3):035425.

[24] Vilatela JJ, Deng L, Kinloch IA, Young RJ, Windle AH. Structure of and stress transfer in fibres spun from carbon nanotubes produced by chemical vapour deposition. Carbon 2011;49(13):4149–58.

[25] Williams G, Watts DC. Non-symmetrical dielectric relaxation behaviour arising from a simple empirical decay function. Trans Faraday Soc 1970;66:80–5.